Dual Reciprocity Boundary Element Method for Steady Infiltration Problems from Furrow Irrigation Channels in Heterogeneous Soil

Muhammad Manaqib*, Yanne Irene, Muhaza Liebenlito, and Rizki Aulia

***Abstract*—This research discusses solving the problem of infiltration of furrow irrigation channels in heterogeneous soil containing five soil layers using the Dual Reciprocity Boundary Element Method (DRBEM) numerical method. The mathematical infiltration model in furrow irrigation channels takes the form of the Richard Equation, which is transformed into a modified Helmholtz equation with mixed boundary conditions. Solving with DRBEM shows that in heterogeneous and homogeneous soils, the soil type influences the suction potential and water content values. Different soil depths in heterogeneous soil produce variations and jumps in suction potential and water content values in each soil layer.**

***Index Terms*—DRBEM; Richard's Equation; Modified Helmholtz Equation; Heterogeneous Soil**

I. Introduction

WATER is a natural resource that has an important role in everyday life. Water availability is always constant due to the hydrological cycle [1]. The large need for water means its availability is limited. This is caused by climate change and increasing population [2]. Good management is needed to overcome this. In this case, it can be done with an irrigation system. The irrigation system is the most important factor in determining harvest success. The working principle of irrigation is to collect water and distribute it to agricultural land. There are 4 types of irrigation systems: surface irrigation, drip irrigation, subsurface irrigation, and bulk irrigation [3]. One application of surface irrigation is furrow irrigation. Apart from the limited water available, other problems are soil salinity and infiltration in the root zone. Areas close to the furrow will be more saturated than areas far from the furrow. Therefore, research is needed to find out. However, this research requires a long time and is expensive because the infiltration process involves soil water content, so the process is difficult to carry out. So an alternative is given by creating a mathematical model [4].

Therefore, several researchers used DRBEM to solve mathematical infiltration models in furrow irrigation channels. Azis et al. [5] examined the Matrix Flux Potential (MFP) values in three-channel shapes, namely flat, circular, and rectangular channels. The research results show that the MFP values for flat and circular channel shapes are almost identical. The MFP value for the rectangular channel shape is greater than the other two channel shapes.

The authors are with the Department of Mathematics, UIN Syarif Hidayatullah Jakarta, Indonesia e-mail: muhammad.manaqib@uinjkt.ac.id

Manuscript received September 27, 2023; accepted February 5, 2025.

Majid et al. [6] investigated trapezoidal irrigation channels on homogeneous soil and concluded that coarser soil generally has higher suction power and produces lower water absorption than fine soil.

Ana et al. [7] examined the suction power and water content values in six-channel shapes, namely flat channels, non-flat watertight channels (rectangular channels, trapezoidal channels), and non-flat channels without watertight (rectangular channels, semicircular channels, trapezoidal channels). The research results show that the suction power value is proportional to the water content value. Sequentially, the order of channel shapes based on highest to lowest water content is non-flat channels without watertight, non-flat channels that are watertight, and flat channels.

Whisler et al. [8] conducted research using heterogeneous scales of hydraulic conductivity with depth. The results obtained depend on the increase in hydraulic conductivity and depth. Solekhudin [9] investigated trapezoidal irrigation channels in heterogeneous soil with 3 soil layers with different depths. The results show a jump in the suction potential value in each soil layer.

Huinong, Ningxia Autonomous Region in Northwest China consists of 5 types of soil with different depths arranged in layers [10]. China has the most dense population in the world, so the needs for daily living are very large, especially in terms of consumption. To obtain satisfactory harvest results, agricultural land with sufficient irrigation is required. Due to limited water availability, climate change, soil salinity problems, and increasing population, water availability has become finite and irrigation systems have been created. Because of these inhibiting factors, research is needed to find out. Transport of water and dissolved substances is needed to overcome this [10].

Based on previous research, DRBEM has been proven effective in solving water absorption problems. So this research aims to find a solution to the problem of infiltration of furrow irrigation channels in heterogeneous soil using the DRBEM numerical method. The heterogeneous soil studied is in the Huinong region, Ningxia Autonomous Region Province, Northwest China, consisting of five different soil layers.

II. METHOD

DRBEM is a method for solving the two-dimensional Helmholtz equation with known boundary conditions. The Helmholtz equation has a domain R, a closed region bounded

by a simple curve C. The general form of the two-dimensional Helmholtz equation is

$$\frac{\partial^2\phi(x,y)}{\partial x^2}+\frac{\partial^2\phi(x,y)}{\partial y^2}+k^2\phi(x,y)=g(x,y) \tag{1}$$

where k is a constant. with boundary conditions

$$\phi=f_1(x,y),\quad (x,y)\in C_1 \tag{2}$$

$$\frac{\partial\phi}{\partial n}=f_2(x,y),\quad (x,y)\in C_2 \tag{3}$$

with C_1 and C_2 is a non-intersecting curve such that $C_1 \cup C_2 = C$.

A fundamental solution is needed to solve the equation (1), However, the solution is difficult and not unique [11]. So the alternative is to solve it with DRBEM because it does not require a fundamental solution of the Helmholtz Equation but simply uses a fundamental solution of the Laplace Equation[14]. The solution with DRBEM is

1) Reciprocal Relation

$$\int_C\left(\Phi\frac{\partial\phi}{\partial n}-\phi\frac{\partial\Phi}{\partial n}\right)ds=\iint_R\Phi\left(g-k^2\phi\right)dxdy$$

2) Boundary Integral Equation in Helmholtz Equation

$$\lambda(\xi,\eta)\phi(\xi,\eta)=$$
$$\int_C\left(\phi(x,y)\frac{\partial\Phi(x,y;\xi,\eta)}{\partial n}-\Phi(x,y;\xi,\eta)\frac{\partial\phi(x,y)}{\partial n}\right)ds$$
$$+\iint_R\Phi(x,y;\xi,\eta)\left(g(x,y)-k^2\phi(x,y)\right)dxdy$$

with

$$\lambda(\xi,\eta)=\begin{cases}0, & \text{if } (\xi,\eta)\notin R\cup C\\ \frac{1}{2}, & \text{if } (\xi,\eta) \text{ lies on a smooth of } C\\ 1, & \text{if } (\xi,\eta)\in R\end{cases}$$

3) Integral Domain Approach with $\rho(x,y;a,b) = 1 + r^2(x,y;a,b) + r^3(x,y;a,b)$

$$\iint_R\Phi(x,y;\xi,\eta)\left(g(x,y)-k^2\phi(x,y)\right)dxdy$$
$$\approx\sum_{m=1}^{M}\beta^{(m)}\iint_R\Phi(x,y;\xi,\eta)\rho\left(x,y;a^{(m)},b^{(m)}\right)dxdy$$

4) Boundary Integral Equations in Line Integrals

$$\lambda(\xi,\eta)\phi(\xi,\eta)=$$
$$\sum_{j=1}^{M}\mu^{(nj)}\left[g\left(a^{(j)},b^{(j)}\right)-k^2\phi\left(a^{(j)},b^{(j)}\right)\right]$$
$$\int_C\left(\phi(x,y)\frac{\partial\Phi(x,y;\xi,\eta)}{\partial n}-\Phi(x,y;\xi,\eta)\frac{\partial\phi(x,y)}{\partial n}\right)ds$$

for $(\xi,\eta)\in R\cup C$.

5) Substitution of Collocation Points into Boundary Integral Equations with System of Linear Equation

$$\lambda\left(\bar{x}^{(n)},\bar{y}^{(n)}\right)\phi\left(\bar{x}^{(n)},\bar{y}^{(n)}\right)$$
$$=\sum_{j=1}^{N+L}\mu^{(nj)}\left[g\left(\bar{x}^{(j)},\bar{y}^{(j)}\right)-k^2\phi\left(\bar{x}^{(j)},\bar{y}^{(j)}\right)\right]$$
$$+\sum_{k=1}^{N}\left[\bar{\phi}^{(k)}{f_2}^{(k)}\left(\bar{x}^{(n)},\bar{y}^{(n)}\right)-\bar{p}^{(k)}f_1^{(k)}\left(\bar{x}^{(n)},\bar{y}^{(n)}\right)\right]$$

for $n=1,2,\ldots,N+L$ with

$$\mu^{(nj)}=$$
$$\sum_{m=1}^{N+L}\omega\left(\bar{x}^{(j)},\bar{y}^{(j)};\bar{x}^{(m)},\bar{y}^{(m)}\right)\psi\left(\bar{x}^{(n)},\bar{y}^{(n)};\bar{x}^{(m)},\bar{y}^{(m)}\right)$$
$${f_1}^{(k)}\left(\bar{x}^{(n)},\bar{y}^{(n)}\right)=$$
$$\frac{1}{4\pi}\int_{C^{(k)}}\ln\left(\left(x-\bar{x}^{(n)}\right)^2+\left(y-\bar{y}^{(n)}\right)^2\right)ds$$
$${f_2}^{(k)}\left(\bar{x}^{(n)},\bar{y}^{(n)}\right)=$$
$$\frac{1}{4\pi}\int_{C^{(k)}}\frac{\partial}{\partial n}\left[\ln\left(\left(x-\bar{x}^{(n)}\right)^2+\left(y-\bar{y}^{(n)}\right)^2\right)ds\right]$$

6) Substitute the solution of linear sytem into the Boundary Integral equation to obtain an equation that can be used to evaluate the PDE at all points in the domain

$$\lambda(a,b)\phi(a,b)=\sum_{j=1}^{N+L}\mu^{(j)}\left[g\left(\bar{x}^{(j)},\bar{y}^{(j)}\right)-k^2\bar{\phi}^{(j)}\right]$$
$$+\sum_{k=1}^{N}\left[\bar{\phi}^{(k)}f_2^{(k)}(a,b)-\bar{p}^{(k)}{f_1}^{(k)}(a,b)\right]$$

with

$$\mu^{(j)}=\sum_{m=1}^{N+L}\omega\left(\bar{x}^{(j)},\bar{y}^{(j)};\bar{x}^{(m)},\bar{y}^{(m)}\right)\psi\left(a,b;\bar{x}^{(m)},\bar{y}^{(m)}\right)$$

$$\lambda(a,b)=\begin{cases}\frac{1}{2} & \text{if } (a,b) \text{ lies on } a \text{ smooth of } C\\ 1 & \text{if } (a,b)\in R\end{cases}$$

$${f_1}^{(k)}(a,b)=\frac{1}{4\pi}\int_{C^{(k)}}\ln\left((x-a)^2+(y-b)^2\right)ds$$

$$f_2^{(k)}(a,b)=\frac{1}{4\pi}\int_{C^{(k)}}\frac{\partial}{\partial n}\left[\ln\left((x-a)^2+(y-b)^2\right)ds\right]$$

III. RESULT AND DISCUSSION

A. Problem Formulation

This research used five types of soil with different depths and arranged in layers. The type of soil used is Regosol soil which has a rough texture with sand content $> 60\%$. Podsol soil has a texture that is not rough and feels slippery[13]. Andosol soil with a finer texture [12]. Sandy Loam and Loamy Sandy represent Regosol soil, Loam A and Loam B represent Podsol soil and Silty Loam represents Andosol soil. Given parameter values for each soil type on Table I.

With assumption [4], the coordinates that will be used are $OXYZ$ where O is the center of the channel, and OZ is

the depth with a positive value. The cross-sectional shape of the irrigation channel does not change along the OY and is symmetrical for $X = \pm k(L+ D), k = 0, \pm1, \pm2, \ldots$, so that the water flow pattern can be assumed to be two-dimensional as in Figure 1. K_0 is the saturated hydraulic conductivity, α

TABLE I: Soil Parameter [10]

Depth (cm)	Soil	K_0 (cm d^{-1})	α (cm^{-1})	n
$0-40$	Sandy Loam	14	0.02	1.35
$40-80$	Loam A	13	0.015	1.39
$80-120$	Loam B	10	0.018	1.35
$120-160$	Silty Loam	7	0.013	1.26
$160-200$	Loamy Sandy	10	0.02	1.25

indicates the roughness of the soil type, θ_r is the residual water content, θ_s is the saturated water content and n is the pore size distribution

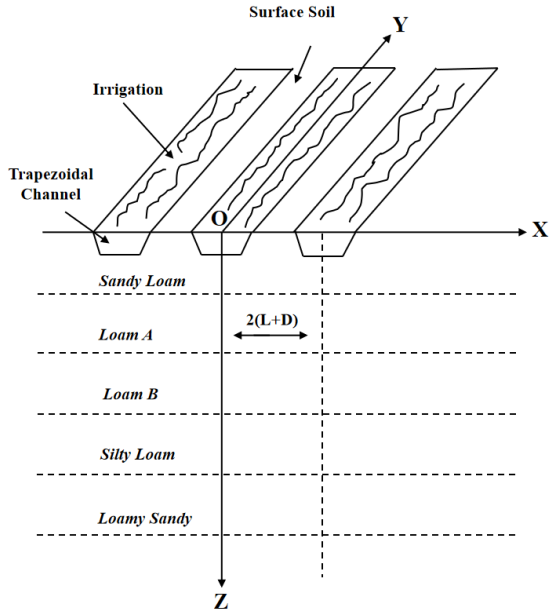

(a) Cross-section of the Furrow Irrigation Channel

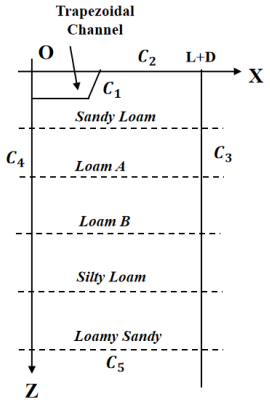

(b) Infiltration Domain in Furrow Irrigation Channel

Fig. 1: Furrow Irrigation Channel

B. Mathematical Models

The following Richard's equation governs steady infiltration in furrow irrigation channels.

$$\frac{\partial\theta}{\partial T} = \frac{\partial}{\partial X}\left(K(\theta)\frac{\partial\psi}{\partial X}\right) + \frac{\partial}{\partial Z}\left(K(\theta)\frac{\partial\psi}{\partial Z}\right) - \frac{\partial K(\theta)}{\partial Z}$$

where K is hydraulic conductivity, ψ is suction potential, and θ is water content.Because Richard's equation is a non-linear differential equation, it will be transformed into a linear form as follows.

1) Kirchoff Transformation

$$\Theta = \int_{-\infty}^{\psi} K(s)ds \tag{4}$$

where Θ is Matrix Flux Potential (MFP) and obtained

$$\frac{\partial\Theta}{\partial X} = K\frac{\partial\psi}{\partial X}$$
$$\frac{\partial\Theta}{\partial Z} = K\frac{\partial\psi}{\partial Z}$$

2) The exponential model of hydraulic conductivity is defined

$$K = K_0 e^{\alpha\psi}, \alpha > 0 \tag{5}$$

Because it is heterogeneous, assume that $\alpha_i, i = 1, 2, ..., 5$ are the values of α in the i-th layer. Based on [9], the value of α can be written

$$\alpha^* = \frac{\alpha_1 + \alpha_2 + \alpha_3 + \alpha_4 + \alpha_5}{5}$$

Substitution (5) to (4) obtained

$$\Theta \Leftrightarrow K = \Theta\alpha^*$$

3) Transformation to dimensionless variables

$$x = \frac{\alpha^*}{2}X, \quad z = \frac{\alpha^*}{2}Z, \quad \Phi = \frac{\pi\Theta}{v_0 L'}$$
$$u = \frac{2\pi}{v_0\alpha^* L}U, \quad v = \frac{2\pi}{v_0\alpha^* L}V, f = \frac{2\pi}{v_0\alpha^* L}F$$

where v_0 is the initial flux and L is half the length of the irrigation channel

4) Transformation with equations

$$\Phi = \phi e^z$$

Thus, we obtain the governing equation of the water infiltration in the furrow irrigation channel in the following linear equation.

$$\frac{\partial^2\phi}{\partial x^2} + \frac{\partial^2\phi}{\partial z^2} = \phi$$

Based on [4], the value of ψ is obtained as the suction potential for irrigation canal infiltration.

$$\psi = \frac{1}{\alpha^*}\ln\left(\frac{\alpha^*\phi e^z v_0 L}{\pi K_0}\right)$$

And the relationship between suction potential and water content is obtained [13].

$$\theta = \left(\frac{1}{1 + (\alpha^*\psi)^n}\right)^m (\theta_s - \theta_r) + \theta_r \tag{6}$$

Based on the assumptions, there is no incoming water flow except at the surface of the irrigation channel, then $F = 0$ for $X = 0, X = L + D$, and $Z = 0$. Assume that at infinite depth, the MFP rate approaches zero so that $\frac{\partial \theta}{\partial X} \rightarrow 0$ for $\frac{\partial \theta}{\partial Z} \rightarrow 0$ for $Z \rightarrow \infty$. So the boundary conditions for the mathematical model of water infiltration in irrigation channels in dimensionless variables are as follows.

$$\frac{\partial \phi}{\partial n} = \frac{2\pi}{\alpha L} e^{-z} + \phi n_2, \text{ on } C_1: \text{ the channel surface,}$$
$$\frac{\partial \phi}{\partial n} = -\phi, \text{ on } C_2: \text{ the ground surface outside the channel,}$$
$$\frac{\partial \phi}{\partial n} = 0, \text{ on } C_3: \text{ for } x = 0 \text{ and } z \geq 0,$$
$$\frac{\partial \phi}{\partial n} = 0, \text{ on } C_4: \text{ for } x = \frac{\alpha}{2}(L + D) \text{ and } z \geq 0,$$
$$\frac{\partial \phi}{\partial n} = -\phi, \text{ on } C_5: \text{ for } 0 \leq x \leq \frac{\alpha}{2}(L + D) \text{ and } z = c.$$

C. Discussion

This study compares the results obtained when the soil in Table 1 is used in homogeneous and heterogeneous soil. The mathematical model obtained in the previous section is then solved using DRBEM, which has been explained in the methodology section. The simulation is carried out using Matlab R2015a software.

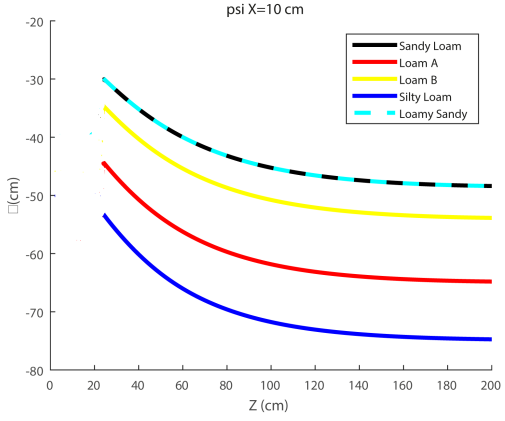

(a) Suction Potential

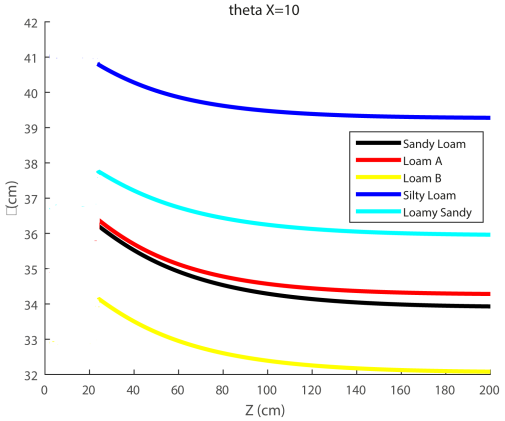

(b) Water Content

Fig. 2: Graph ψ and θ along $X = 10$

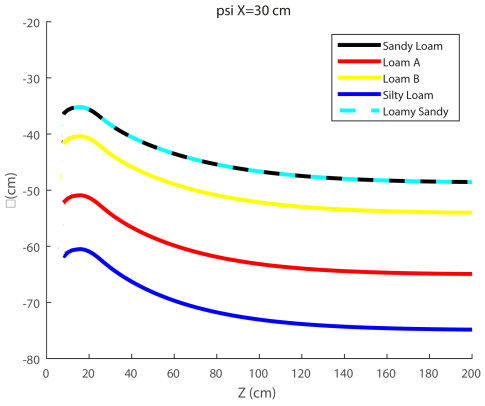

(a) Suction Potential

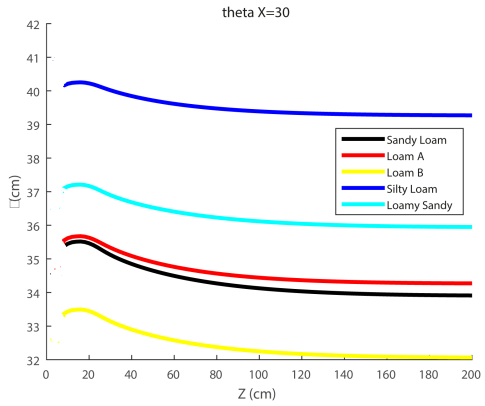

(b) Water Content

Fig. 3: Graph ψ and θ along $X = 30$

Figures 2 to 6 show the values of suction potential and water content evaluated at $X = 10, 30, 50, 70, 90; 0 \leq Z \leq 200$, inhomogeneous soil. Based on Figure 2 and Figure 3, graph ψ and θ along the axes $X = 10$ and $X = 30$ indicate that the soil is below the water channel and the values of ψ and θ decrease as the depth increases. It can be concluded that the suction potential value is assumed to be directly proportional to the water content. The water content in shallow locations will be greater than in deeper locations in the soil below the channel. This is because water seeps into deeper soil below the channel.

Based on Figure 4 - Figure 6, The values of ψ and θ along the lines $X = 50, X = 70$ and $X = 90$ indicate that the soil not under irrigation channels. This is because as the depth increases, the graphs of ψ and θ move towards the point of convergence. However, the relationship pattern for each type of soil is different. The θ value at a shallow location will be smaller than at a deep location where the soil is not under the channel. It can be concluded that the water enters the ground surface because the water only enters through channels.

Next, we will discuss the 5 layers of heterogeneous soil presented in Figure 7. The value of ψ for $X = 10$ in each soil layer has the highest value compared to other X. Meanwhile, $X = 90$ in each soil layer has the lowest value compared to other X values. So it can be said that the highest value of suction potential (ψ) is closest to the channel while the lowest

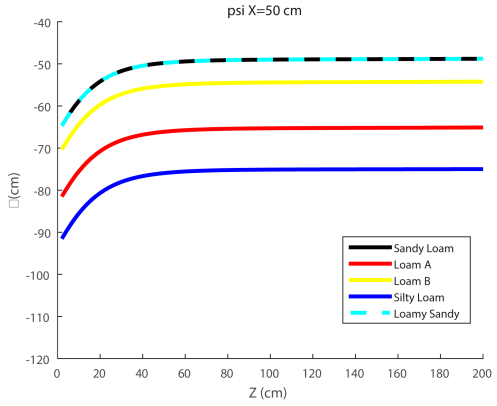

(a) Suction Potential

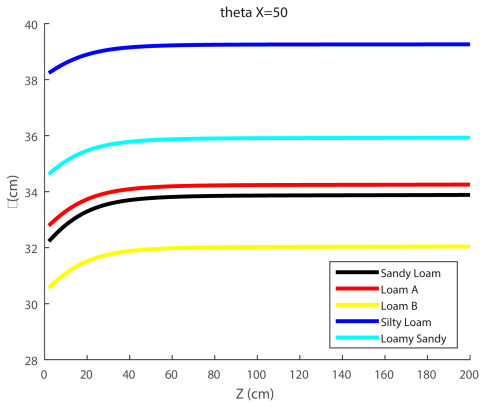

(b) Water Content

Fig. 4: Graph $\boldsymbol{\psi}$ and $\boldsymbol{\theta}$ along $\boldsymbol{X = 50}$

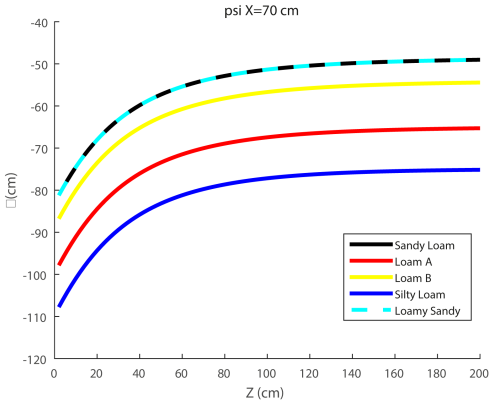

(a) Suction Potential

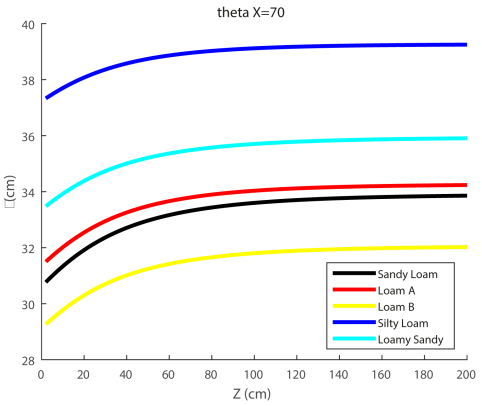

(b) Water Content

Fig. 5: Graph $\boldsymbol{\psi}$ and $\boldsymbol{\theta}$ along $\boldsymbol{X = 70}$

value of suction potential (ψ) is at the location farthest from the ground surface.

Based on Figure 7, in the first, second, and third soil layers for $X = 10, X = 30, X = 50, X = 70$, and $X = 90$, there are variations in the values of ψ and θ for different depth point. Meanwhile, in the fourth layer, there is no clear variation in the values of ψ and θ, and in the fifth layer, there is almost no variation in the values of ψ and θ.

There is a jump in the value of ψ for $0 \leq Z \leq 40$, to $40 \leq Z \leq 80$, because there are differences in soil types in the two layers. Likewise, with the jump in ψ values for $80 \leq Z \leq 120, 120 \leq Z \leq 160$ and $160 \leq Z \leq 200$ It can be concluded that the first soil layer produces the highest ψ value and the fourth soil layer produces the lowest ψ value.

Based on Figure 7, the largest water content is in the fourth soil layer (Silty Loam), meaning that this type of soil can hold water so that water does not seep into the soil layer beneath it but to the side of the channel. Meanwhile, the smallest water content is in the first soil layer, this is because sandy soil has a high water suction capacity so that water in the first soil layer will seep into the second soil layer. From the explanation above, it can be concluded that ψ is directly proportional to θ. In heterogeneous soil, if the n and K_0 values are greater, the suction potential value will also be greater.

A surface plot is given to see the distribution of values. ψ and θ. Based on Figure 8 - Figure 12, The highest suction potential value is at the bottom of the channel, and the smallest value is at the ground surface outside the channel at the farthest distance from the center of the channel. It can be seen that the distribution pattern of suction potential values is almost the same. It can be seen that the suction potential value in this domain is Sandy Loam between -40 cm to -90 cm, Loam A between -50 cm to -100 cm, Loam B between -40 cm to -80 cm, Silty Loam between -60 cm to 110 cm Loamy Sandy between -40 cm to -85 cm.

The water content values in this domain are Sandy Loam between 30% to 36%, Loam A between 31% to 37%, Loam B between 29% to 34%, Silty Loam between 38% to 40% and Loamy Sandy between 34% to 37%. This indicates that the soil types containing the most water are Silty Loam, Loamy Sandy, Loam A, Sandy Loam, and Loam B.

Next, a surface plot is given on heterogeneous soil. Based on Figure 13, the first layer of soil below the channel has a large ψ value, whereas when it is on the ground surface outside the channel, it has a low ψ value. This is the same as the second and third soil layers. The fourth soil layer has the lowest ψ and largest θ values compared to other soil layers. This strengthens the assumption that the suction potential value is proportional to the water content.

The suction potential values in this domain are Sandy Loam between -30 cm to 75 cm, Loam A between -65 cm to -90 cm, Loam B between -50 cm to -60 cm, Silty Loam

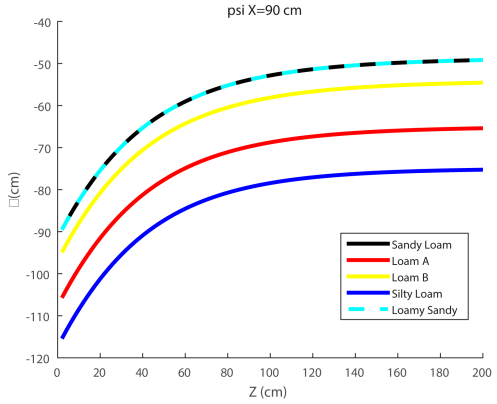

(a) Suction Potential

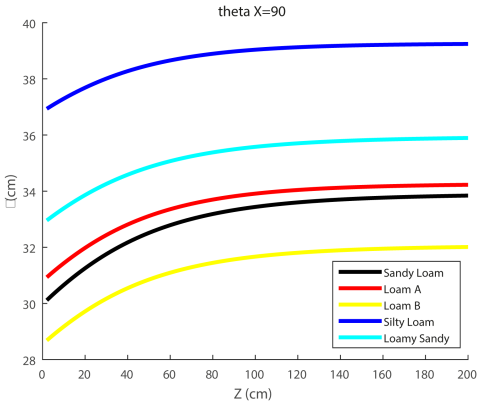

(b) Water Content

Fig. 6: Graph ψ and θ along $\boldsymbol{X = 90}$

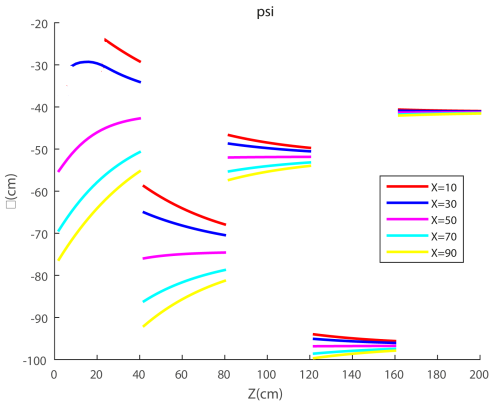

(a) Suction Potential

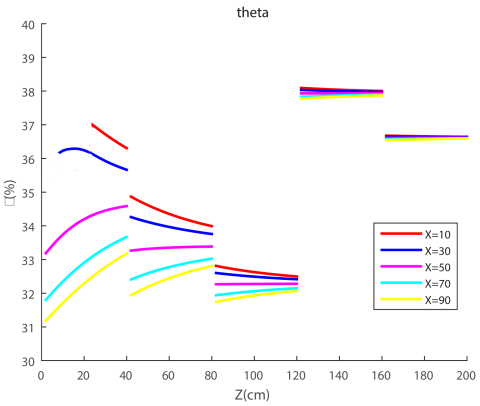

(b) Water Content

Fig. 7: Graph of ψ and θ in Heterogeneous Soil

between -96 cm to -100 cm Loamy sandy between -40 cm to -41 cm. The water content values in this domain are Sandy Loam between 32% to 36.5%, Loam A between 31% to 33.5%, Loam B between 31% to 32%, Silty Loam between 37% to 37.5% and Loamy Sandy between 36% to 36.5%.

IV. CONCLUSION

DRBEM can solve the problem of infiltration of furrow irrigation channels in heterogeneous soil by using a governing equation, namely the Richard equation, which is transformed into a modified Helmholtz equation with mixed boundary conditions.

In heterogeneous soil, the results show an influence of soil type on suction potential and water content. Soil with many pores and large hydraulic conductivity will produce a large suction potential. The results of homogeneous soil show that soil type influences suction potential and water content. Soil with a large α will produce a large suction potential. This is directly proportional to water content.

The depth of heterogeneous soil for each different soil type also influences the soil's suction capacity and water content. When at a depth of 0 cm to 40 cm, a depth of 40 cm to 80 cm and a depth of 80 cm to 120 cm, the soil has varying suction potential and water content values. However, when the soil depth increases, namely at a depth of 120 cm to 160 cm, the variation in values is still visible but small, and at a depth of

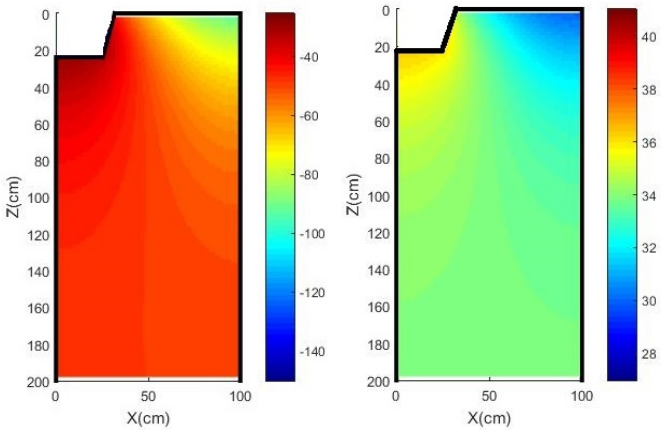

(a) Suction Potential (b) Water Content

Fig. 8: Surface Plot ψ and θ on Sandy Loam

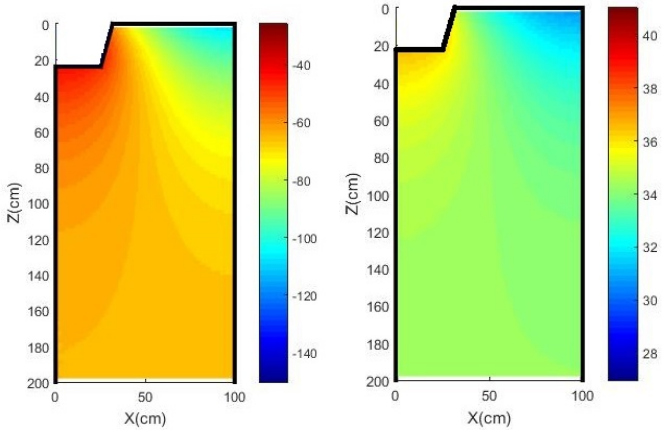

(a) Suction Potential (b) Water Content

Fig. 9: Surface Plot ψ and θ on Loam A

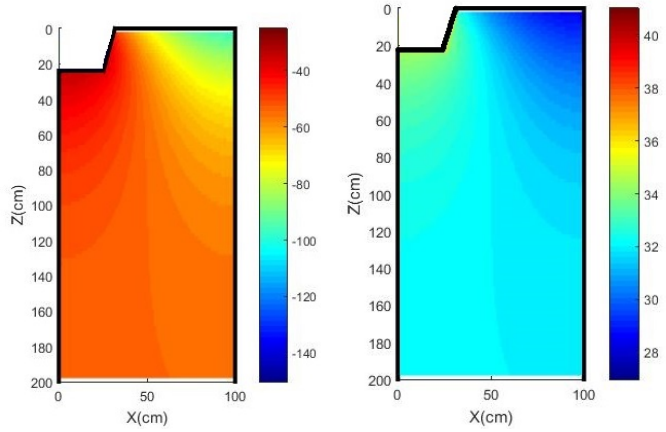

(a) Suction Potential (b) Water Content

Fig. 10: Surface Plot ψ and θ on Loam B

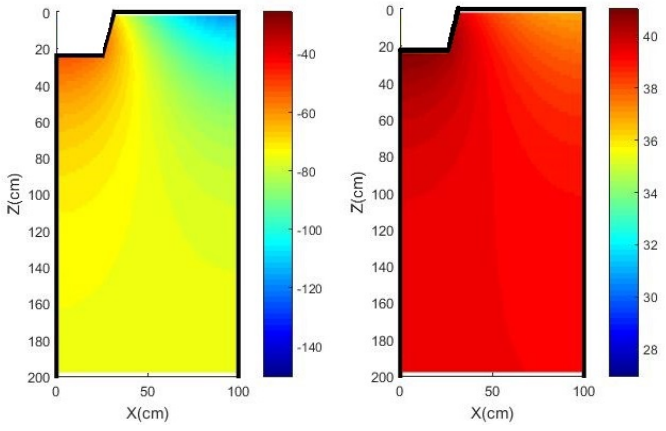

(a) Suction Potential (b) Water Content

Fig. 11: Graph of ψ and θ in Silty Loam

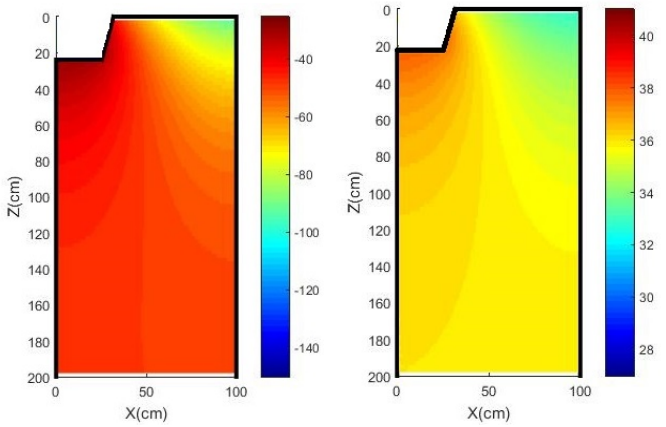

(a) Suction Potential (b) Water Content

Fig. 12: Graph of ψ and θ in Loamy Sandy

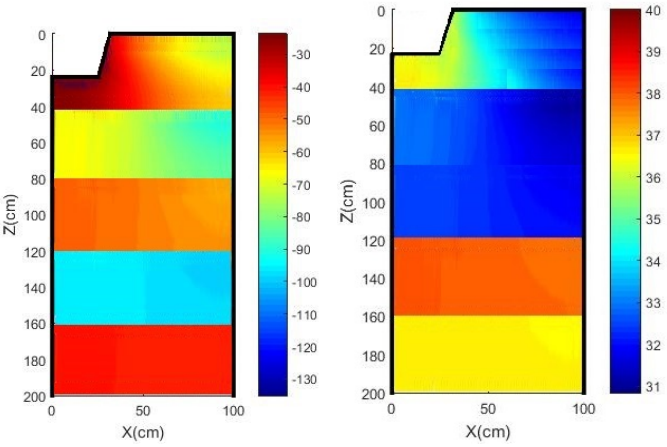

(a) Suction Potential (b) Water Content

Fig. 13: Surface Plot ψ and θ on Heterogeneous Soil

160 cm to 200 cm there is almost no variation in the suction potential and water content values. Differences in soil types in heterogeneous soil result in jumps in values between soil layers.

REFERENCES

[1] Haris and Kaharuddin, "Agrohidrologi," Badan Penyuluhan dan Pengembangan SDM Pertanian Kementerian Pertanian, 2018, p. 122.

[2] C. Samekto and E. S. Winata, "Potensi Sumber Daya Air di Indonesia," in Seminar Nasional Aplikasi Teknologi Penyediaan Air Bersih untuk Kabupaten/Kota di Indonesia, Indonesia, 2016.

[3] R. B. Rosadi, "Dasar - Dasar Teknik Irigasi," Yogyakarta, Graha Ilmu, 2015, pp. 13-14.

[4] M. Manaqib, "Pemodelan Matematika Infiltrasi Air pada Saluran Irigasi Alur," JURNAL MATEMATIKA "MANTIK", vol. 03, no. 01, 2017.

[5] M. I. Azis, D. L. Clements and M. Lobo, "A BOundary Element Method For Steady Infiltration From Periodik Channels," AZIAM J, pp. 61-78, 2003.

[6] N. Inayah, M. Manaqib and W. N. Majid, "Furrow Irrigation Infiltration in Various Types Using Dual Reciprocity Boundary Element Method," in AIP Conference Proceedings, 2021.

[7] A. Nurhasanah, M. Manaqib and I. Fauziah, "Analysis Infiltration Waters in Various Forms of Irrigation Channels by Using Dual Reciprocity Boundary Element Mrthod," Jurnal Matematika MANTIK, vol. 6, no. 1, pp. 52-65, 2020.

[8] F. D. Whisler, K. K. Watson and S. J. Perrens, "The Numerical Analysis of Infiltration into Heterogeneous Porous Media," in Soil Society of America Proccedings, USA, 1972.
[9] I. Solekhudin, "Steady Infiltration in Heterogeneous Soil," Journal of Physics, 2018.
[10] S. Chen, X. Mao, D. A. Barry and J. Yang, "Model of Crop Growth, Water Flow and Solute Transport in Layered Soil," Agricultural Water Management, pp. 160-174, 2019.
[11] J. T. Katsikadelis, Boundary Elements : Theory And Application, UK: Elsevier, 2002.
[12] J. Gunawan, R. Hazriani and R. Y. Mahardika, Buku Ajar Morfologi dan Klasifikasi Tanah, Pontianak: researchgate, 2020.
[13] A. W. Warrick, Soil Physics Companion, Washington DC: CRC Pres LLC, 2002.
[14] M. Lobo, Boundary Element Methods For The Solution Of A Class Of Infiltration Problems, Australia: University of Adelaide, 2008.